Available online at www.sciencedirect.com
SCIENCE DIRECT®

Journal of the European Ceramic Society 24 (2004) 3043–3048

www.elsevier.com/locate/jeurceramsoc

Synthesis, characterization and properties of nano-sized $SrBi_2Ta_2O_9$ ceramics prepared by chemical routes

Asit. B. Panda, Abhijit Tarafdar, Panchanan Pramanik*

Department of Chemistry, Indian Institute of Technology, Kharagpur 721302, West Bengal, India

Received 24 January 2003; received in revised form 8 July 2003; accepted 19 July 2003

Abstract

Nano-crystalline Strontium Bismuth Tantalate (SBT) has been synthesized by four different chemical based solution methods using metal salts, EDTA, triethanolamine, poly-vinyl alcohol, sugar and ammonium tartarate. The particle size of the synthesized powder was found to be in the range of 15–85 nm, depending on the nature of the precursor solution. The method using tartarate, triethanolamine and EDTA as complexing agents gave the smallest particle size of 15 nm. Bi-evaporation has been prevented totally through efficient low temperature sintering and more than 97% sintered density has been achieved after sintering at 950 °C for 4 h, the product exhibited a dielectric constant of 1387.
© 2003 Published by Elsevier Ltd.

Keywords: Citrate; Dielectric properties; Nanopowders; Polyvinyl alcohol; Sintering; $SrBi_2Ta_2O_9$; Tartarate; Triethanolamine

1. Introduction

The most attractive feature of strontium bismuth tantalate (SBT) is its application in non-volatile ferroelectric random access memories (NVFRAM), which may replace the silicon based, electrically vulnerable programmable read only memories as they posses low operating voltage, high reading and writing speed and nonvolatility.[1–5] It also has excellent fatigue endurance even after 10^{12} cycles of operation,[6,7] low leakage current and low operating voltage. Lead zirconate titanate (PZT), another promising material for the application in NVFRAM, has the major drawback that it suffers severe polarization fatigue on platinum electrodes after long switching cycles. The structure of SBT, a layered type perovskite ferroelectric,[8] consists of perovskite like $[TaO_6]^{7-}$ octahedron layers and $(Bi_2O_2)^{+2}$ layers, with the strontium cations located in the space between the $[TaO_6]^{7-}$ octahedron.[9] The spontaneous polarization arises from the $[SrTaO_3]$ group, which lies parallel to the $[Bi_2O_3]^{2+}$ layers, since the $[Bi_2O_3]^{2+}$ layers weaken the dipole interaction of the perovskite building block.[10] Several research groups have investigated the synthesis of SBT powder or SBT films. The latter have been reported to be prepared by physical vapor deposition (PVD),[11–16] metal organic deposition (MOD),[17–19] metal organic chemical vapor deposition (MOCVD)[20] or sol-gel techniques.[10, 21] But there is limited literature on the preparation and characterization of SBT powders. In the powder synthesis, chemical processes ensure chemical homogeneity and stoichiometric control through molecular level mixing of the starting materials in a solution.[22,23] Among the chemical processes, sol-gel[24,25] and colloid emulsion[26] method are most promising, but they require metal alkoxides or metal halides, which are inconvenient to use due to their moisture sensitivity and high cost.

Alternative aqueous based chemical processes are difficult to find, as the salts of Vb group metals are difficult to make water-soluble. However the use of water-soluble coordinating complexes of the Vb group metals has been reported recently.[27,28] These starting materials are stable in aqueous medium.

In this present paper, we report an aqueous solution based chemical process for the synthesis of nano-crystalline powders of $SrBi_2Ta_2O_9$ from readily available raw materials, which involves an aqueous solution of coordinated metal ions. Coordinating/complexing agents like triethanolamine, ammonium tartarate and

* Corresponding author. Tel.: +91-3222-55303.
E-mail address: asitp@chem.iikgp.ernet.in (A.B. Panda).

0955-2219/$ - see front matter © 2003 Published by Elsevier Ltd.
doi:10.1016/j.jeurceramsoc.2003.07.006

citrate are used to keep the constituent metal ions in homogeneous solution. Dehydration and decomposition of the aqueous solution mixture, followed by calcination produce nano-sized SBT powder, which was characterized by thermal analysis (DTA and TG), X-ray diffractometry and TEM. The sintering behavior of the nano-sized SBT powder is investigated. In addition, the dielectric properties of the sintered pellets (sintered at different temperature) have been studied.

1.1. Experimental work

Tantalum oxide (Ta_2O_5) (Aldrich, 99.8%) was digested in HF (Merck, India) (1:14 mole ratio) to make a water-soluble tantalum-complex due to the formation of water-soluble $[TaOF_5]^{2-}$ and/or $[TaF_7]^{2-}$ species. Addition of ammonium oxalate (Aldrich 99 + %) followed by dilute ammonia-solution to that clear solution results in an insoluble hydrous tantalum hydroxide (Ta_2O_5, nH_2O). This residue was washed thoroughly with 5% ammonia-solution to remove fluoride ions. After assay of Ta_2O_5, the hydrous Ta_2O_5 was digested in ammonium tartarate (Aldrich, 99%) (4 mol) and ammonium citrate (Aldrich, 98%) (4 mol) solution separately to make tantalum tartarate and tantalum citrate respectively through constant stirring at about 40 h. The addition of a catalytic amount of H_2O_2 (Merck, India) (2–5 mol%) enhances the rate of dissolution of the metal ions several folds. The overall process is shown in Fig. 1.

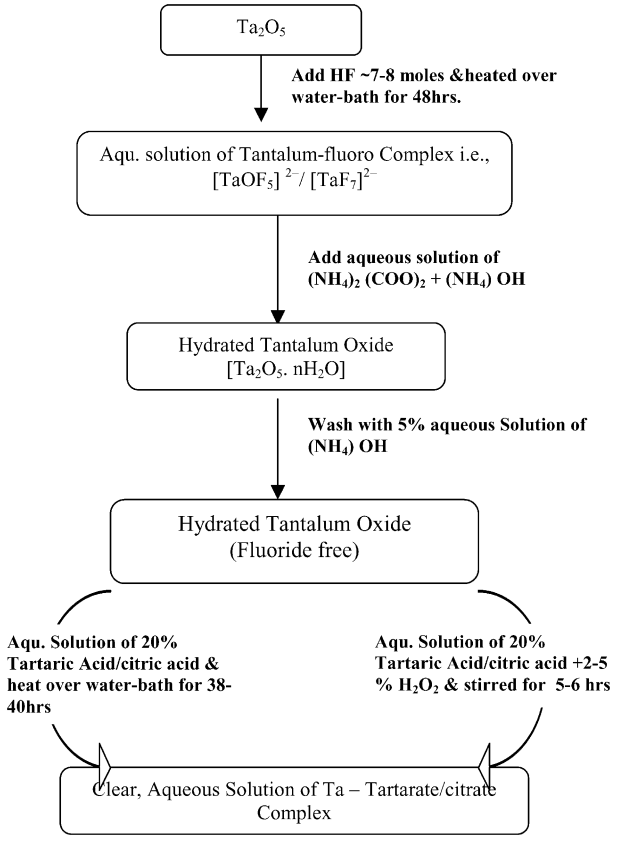

Fig. 1. Schematic representation of the preparation of the aqueous solution of tantalum tartarate/citrate complex.

Strontium–EDTA complex was prepared by mixing an ammoniacal aqueous solution of EDTA (1M) (Aldrich, 99.5%) with aqueous strontium nitrate (SRL, India) solution. The bismuth-TEA complex was made by mixing TEA (MERCK, India, 99%) (2M) with aqueous Bismuth nitrate solution (SRL, India)

1.2. Preparation of SBT

Four methods are adopted to synthesize nano-sized SBT. These are as follows.

1.2.1. Tartarate–TEA process

Stoichiometric amounts of Sr–EDTA, Bi–TEA and Ta–tartarate were mixed together, followed by addition of excess TEA (4 mol with respect to the total metal ion) resulting in a clear precursor solution.

1.2.2. Citrate–TEA process

Stoichiometric amounts of Sr–EDTA, Bi–TEA and Ta-citrate were mixed together, followed by addition of excess TEA (4 mol with respect to the total metal ion) resulting in a clear precursor solution.

1.2.3. Tartarate–PVA–sugar process

Stoichiometric amounts of Ta–tartarate, Sr–nitrate and Bi–nitrate solution were mixed together to get a clear solution. Sugar (no. of moles of sugar $= 3 \times$ no of moles of metal ion) and 10% PVA solution (no. of moles of monomer of PVA $= 2 \times$ no of moles of metal ion) were added to it and mixed well to make the precursor solution.

1.2.4. Citrate–PVA–sugar process

Stoichiometric amounts of Ta–citrate, Sr–nitrate and Bi–nitrate solution were mixed together to get a clear solution. Sugar and 10% PVA solution as in process C.

A fluffy, mesoporous-carbon rich precursor mass was produced by heating the precursor solutions at about 200 °C for complete evaporation of the water. Subsequent calcination of the precursor material results in nano-sized SBT powders. The precursor material and final product have been investigated through thermal studies (DTA and TG) using a Shimadzu DT-40 thermal analyzer, by room temperature powder X-ray diffractometry (XRD) with $CuK_{\acute{a}}$ radiation using a Phillips PW 1710 system, by transmission electron microscopy (TEM) using a model TM 300, Phillips, and dielectric properties by using a capacitance-measuring assembly (model AP-1620, GRC) on sintered pallets have been measured. The chemical compositions have been analyzed by EDAX.

2. Results and discussions

The flow diagram (Fig. 1) is based on our previous reported synthesis of the niobium tartarate complex.[28] Precipitated hydrated poly-nuclear tantalum oxides are difficult to dissolve in ammonium tartarate. Addition of a complexing agent, such as ammonium oxalate before precipitation of the tantalum hydroxide from the tantalum fluoride complex solution, helps to reduce poly-nuclear chain formation during precipitation of the tantalum hydroxide.[29] Thus, the addition of ammonium oxalate helps to reduce the number of hydroxy or oxo bridges of the hydrated tantalum oxide. This hydrous tantalum oxide is soluble in tartaric acid/citric acid. In the presence of H_2O_2, the hydrous tantalum oxide produces a soluble yellow per-oxo complex [30] that enhances the rate of solubility of hydrous tantalum oxide in ammonium tartarate/ammonium citrate.

Complete evaporation of the starting precursor solution (~200C) leads to the decomposition of the metal-complexes and excess TEA. The entire process was accompanied by the evolution of gases such as: CO, CO_2, NH_3, NO_2 and water vapor, which facilitated the formation of a carbon-rich, fluffy and highly porous structure with tap density 0.3 gm/cc. The BET surface area of the generated carbonaceous mass was found to be high, ranging between 150 and 175 m^2/gm, which implied that the precursor material was essentially a matrix of mesoporous carbon. This was confirmed by the TEM studies indicating a pore-size of 40–50 nm.

Simultaneously recorded thermal gravimetric (TG) and differential thermal gravimetric (DTG) studies of the precursor powder were carried out in air at a heating rate of 10 °C/min. Fig. 2 illustrates the thermogram of the SBT precursor powder prepared by the tartarate TEA process as a typical example. The precursor powders may be considered to be constituted from the metal carboxylate and the respective metal oxide trapped in a pyrolyzed mass. The general thermograms reveal a strong exothermic peak between 300 and 500 °C accordingly the evolution of large amounts of gas, resulting in major weight loss in the TG curve. The evolution of the various gasses not only helps the precursor material to disintegrate but also to dissipate the heat of decomposition, thus inhibiting agglomeration and sintering of the fine particle. The heat treatment temperature significantly influences the reactivity and particle size.

To study the effect of heat-treatment temperature on the layer-perovskite phase formation, XRD of the calcined mass (at different temperatures ranging from 500–900 °C/2 h) was performed. The XRD of some calcined SBT powders and their precursor powders, made by tartarate–TEA and citrate–TEA method are shown in Fig. 3. Room temperature X-ray diffractographs revealed the virgin precursor powder *to be* amorphous in nature. Thermal treatment of the precursor powders at 500 to 650 °C revealed the formation of a fluorite–SBT phase;[27] the appearance of the perovskite SBT phase was observed to occur after 650 °C. Calcination at 700–800 °C/2 h shows that the fluorite phase totally transforms into perovskite SBT phase. Since the crystallization of the final layered perovskite phase from the virgin precursors was observed to occur via a Fluorite–SBT phase, this phase could be considered to be the nucleating phase for the formation of the final SBT-phase. The crystallite sizes in the calcined powders have been calculated from X-ray line broadening studies using the Scherer equation [31] and were found in the range of 12–21 nm.

The finer details of the particles and their morphology were investigated by TEM. The bright field electron micrographs of the calcined powders, heat-treated at different temperatures, reflected the basic powder morphology, where the smallest visible particle could be identified as the crystallite and/or their agglomerates. The corresponding selected area electron diffraction (SAED) pattern of the particles showed distinct rings, suggestive of an assembly of nanocrystallites. Typical bright field micrographs and SAED patterns of SBT

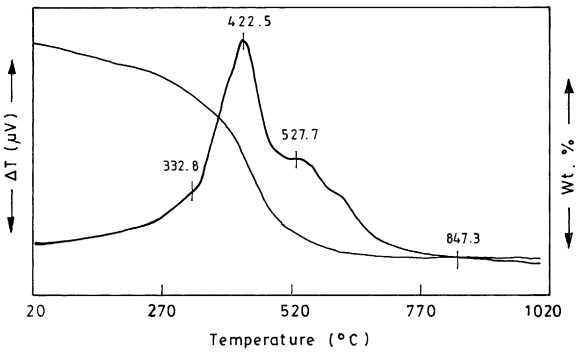

Fig. 2. Thermal studies of the $SrBi_2Ta_2O_9$ precursors powders prepared by tartarate–TEA process.

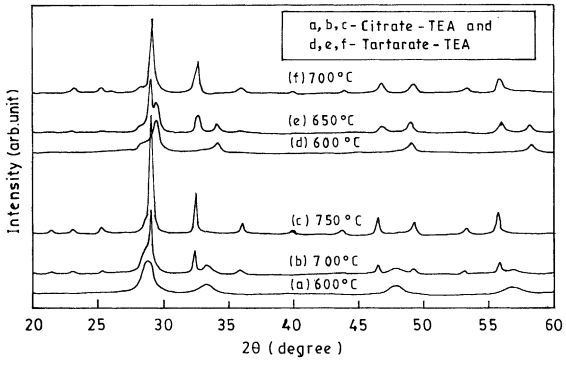

Fig. 3. The X-ray diffractograms (using CuK radiation) of calcined (atAdifferent temperature for 2 h) $SrBi_2Ta_2O_9$ precursors prepared by tartarate–TEA and citrate–TEA process.

powders, obtained from the tartarate–TEA process, are shown as a typical representative example in Figs. 4 and 5 respectively. Table 1 summarizes the average particle and crystallite sizes of the materials, as obtained by TEM and XRD analysis respectively. XRD and TEM studies have shown that the X-ray crystallite sizes were comparable (ranging 12–21) for the SBT samples prepared by different solution based chemical methods, but the particle sizes were different (ranging 15–86), which indicates that the particles are agglomerated with different degrees of agglomeration.

The calcined SBT nano-crystalline powder was compacted into pellets by applying a uni-axial pressure of 3.2×10^7Pa and was then sintered at 950 °C/4 h. Density measurements of the sintered SBT pellets were carried out using the Archimedes method and were found to be 97.6% of the theoretical density for only the pellet made by the powders from the Tartarate–TEA route. The other three pellets (made by citrate–TEA, tartarate–PVA–sugar and citrate-PVA–sugar route powder) show poorer sintered density, which have been shown in Table 1. Both sides of the sintered pellets were polished and electroded by applying silver paste. Studies of the variation of the dielectric constant (ϵ) with temperature at a constant frequency of 100 kHz have been performed. Due to the poor density of the pellets made by the citrate–TEA, tartarate–PVA–sugar and Citrate–PVA–sugar methods, those exhibit poor dielectric properties. They were therefore sintered at higher temperature ($\leqslant$1100 °C/4h.) to get maximum density and their dielectric properties were then measured (Table 2).

It is well established that the sintering of SBT pellets, at high sintering temperature is associated with Bi-loss.[33] To depress Bi-loss through evaporation, excess Bi_2O_3 is often used.[32] The sintering of powders produced by the processes tartarate–TEA and citrate–TEA did not show any Bi loss from the pallets due to the lower sintering temperature. The analyses of the sintered pallets

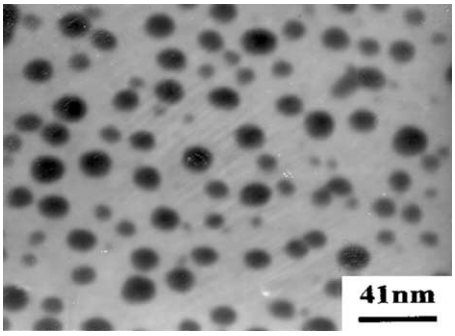

Fig. 4. Bright field transmission electron micrograph of the $SrBi_2Ta_2O_9$ samples after calcination of the precursor powders at 700 °C/2 h obtained from tartarate–TEA process.

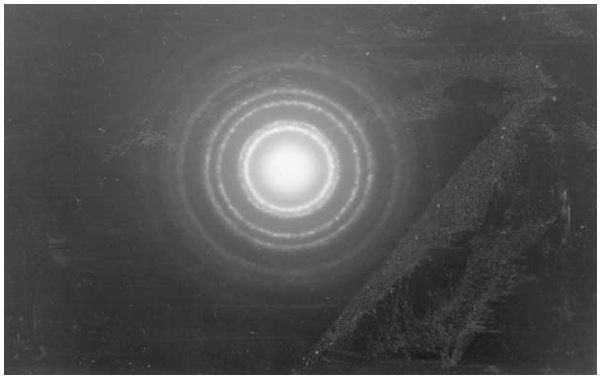

Fig. 5. The corresponding selected area electron diffraction (SAED) pattern of the $SrBi_2Ta_2O_9$ powders after calcination of the precursor powders at 700 °C/2 h obtained from tartarate–TEA process.

Table 1
Comparison of general characteristics of synthesized SBT ceramics

Sample	Calcination temperature (°C)	Average crystallite size (nm)	Average particle size (nm)	Relative density of pallets at sintering temperature 950 °C	T_C (°C) (±2 °C)	$\epsilon_{max.}$ (±100)
Tarterate–TEA	700	12	15	97.6	279	1387
Citrate–TEA	750	17	19	96.4	283	1232
Tarterate–PVA–sugar	750	16	35	94.9	280	988
Citrate–PVA-sugar	800	21	86	91.7	275	546

Table 2
Variation of dielectric properties with sintering temperatures of synthesized SBT ceramics by four different synthesis route

Sample	Sintering temperature (°C)	Relative density	Dielectric constant (±100)	T_C (°C) (±2 °C)
Tarterate-TEA	950	97.6	1387	279
Citrate–TEA	1000	97.4	1344	283
Tarterate-PVA-Sigar	1050	97.1	837	286
Citrate- PVA-Sigar	1100	97.7	461	285

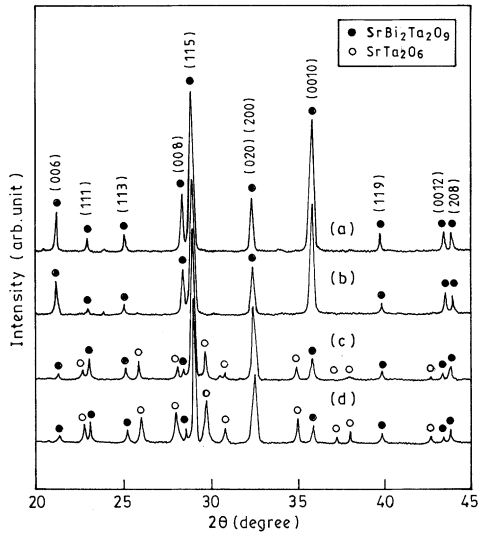

Fig. 6. The X-ray diffractograms (using CuK radiation) of the maximum dense $SrBi_2Ta_2O_9$ sintered pellets sintered at the temperature (a) 950 °C for TEA-tartarate (b) 1000 °C for TEA-citrate (C) 1050 °C for tartarate–PVA–sugar and (d) 1100 °C for citrate- PVA–sugar processes.

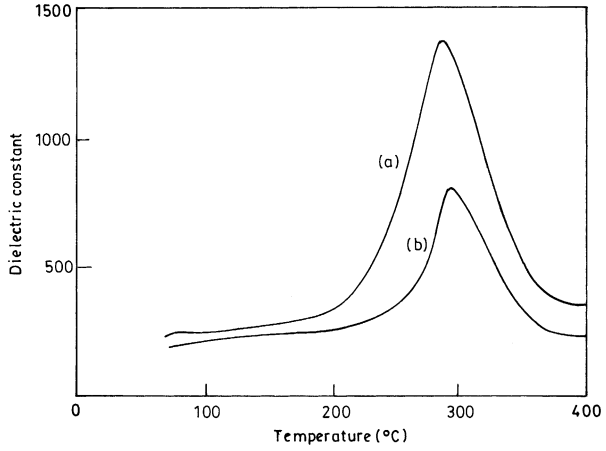

Fig. 7. Variation of dielectric constant (ϵ) with temperature for maximum dense SBT palates (a) $SrBi_2Ta_2O_9$ from TEA-tartarate process and (b) $SrBi_2Ta_2O_9$ from tartarate–PVA–sugar process.

were done by X-ray Diffraction (Fig. 6) and EDAX, which showed no noticeable change in chemical composition. However, the other two maximum dense sintered pellets (powder prepared by Tartarate–PVA–sugar and Citrate–PVA–sugar route) show the Bi-loss due to the higher sintering temperature.

The dielectric constants (Table 2) initially increase gradually with temperature and attain maxima (ϵ_{max}) at the Curie temperature (T_c), as in normal in ferroelectric materials. Due to Bi evaporation, the dielectric constant for the citrate–PVA–sugar product decreases drastically. Fig. 7 shows the corresponding variation of dielectric constant of SBT obtained from the tartarate–TEA and tartarate–PVA–sugar methods. It is observed that SBT powders, prepared through tartarate–TEA precursor have the highest dielectric constant (1387) after sintering at 950 °C/4 h at a Curie temperature 279 °C which is very close to the reported value[33] (290 °C). The ϵ_{max} is higher than that reported [33] (500).

3. Conclusion

Crystallite sizes of the synthesized powder, prepared by different routes, are comparable (ranging 12–21); however, the particle sizes are different, ranging between 15 and 86 depending on the composition of solutions. Bi-evaporation has been minimized and more than 97% of sintered density has been achieved at a sintering temperature less than 1000 °C for 2 h using the tartarate–TEA and citrate–TEA precursor solutions. It has been observed that SBT powders, prepared through tartarate–TEA precursor have a high dielectric constant 1387 after sintering at 950 °C/2 h at a Curie temperature of 279 °C.

References

1. de Araujo, C. A. P., Cuchiaro, J. D., McMillan, L. D., Scott, M. C. and Scott, J. F., Fatigue free ferroelectric capacitors with platinum electrodes. *Nature (London)*, 1995, **374**, 627–629.
2. Jones, R. E. Jr., Maniar, P. D., Moazzami, R., Zurcher, P., Witowski, J. Z., Lii, Y. T., Chu, P. and Gillespie, S. J., Ferroelectric non-volatile memories for low voltage, low powder applications. *Thin Solid Flims*, 1995, **270**(1–2), 584–588.
3. Jones, R. E. Jr. and Desu, S. B., Process integration for non-volatile memory application. *Mater. Res. Soc. Bull.*, 1996, **21**(6), 55–58.
4. Al-Shareef, H. N., Kington, A. I., Chen, X., Bellur, K. R. and Auciello, O., Contribution of electrodes and micro-structures to the electrical properties of $Pb(Zr_{0.53}Ti_{0.47})O_3$ thin film capacitors. *J. Mater. Res.*, 1994, **9**(11), 2968–2975.
5. Kushida-Abdelghafar, K., Miki, H., Yano, F. and Fuzisaki, Y., IrO_2/Pb(Zr_xTi_{1-x})O3(PZT)/Pt ferro-electric thin film capacitor resistant to hydrogen-annealing damage. *Jpn. J. Appl. Phys.*, 1997, **36**(8A), 1032–1034.
6. Scott, J. F., Ross, F. M., De Araujo Paz, C. A., Scott, M. C. and Hoffman, M., Structure and device characteristics of $srbi_2ta_2o_9$ based nonvolatile random access memories. *M.R.S. Bull.*, 1996, **21**, 33–39.
7. De Araujo Paz, C. A., Cuchiaro, J. D., Scott, M. C. and McMillan, L. D., Layered superlattice material applications background of the inventions. *International Patent*, 1993, WO93, 12542.
8. Aurivillus, B., Mixed bismuth oxides with layer lattices, 1. The structure type of $CaNb_2Bi_2O_9$. *Arkiv für kemi*, 1949, **54**, 480–483.
9. Subbarao, E. C., A family of ferroelectric bismuth compounds. *J. Phys. Chem. Solids*, 1962, **23**, 665–676.
10. Kato, K., Zheng, C., Finder, J. M., Dey, S. K. and Torii, Y., Sol-gel rout to ferroelectric layer-stractured perovskite $SrBi_2Ta_2O_9$ and $SrBi_2Nb_2O_9$ thin films. *J. Am. Cerm. Soc.*, 1998, **81**(7), 1869–1875.
11. Park, S. S., Yang, C. H., Yoon, S. G., Ahn, J. H. and Kim, H. G., Characterization of ferroelectric $SrBi_2Ta_2O_9$ thin films deposited by a radio-frequency magnetron sputtering technique. *J. Electrochem. Soc.*, 1997, **144**(8), 2855–2858.
12. Song, T. K., Leem, J. K. and Jung, H. J., Structural and ferroelectric properties of the C-axis oriented SBT thin films deposited by the radio-frequency magnetron sputtering. *Appl. Phys. Lett.*, 1996, **69**(25), 3839–3841.

13. Lee, J. K., Jung, H. J., Aucielto, O. and Kingon, A. I., Electrical characterization of $Pt/SrBi_2Ta_2O_9/Pt$ capacitors fabrication by the pulsed laser ablated deposition technique. *J. Vac. Sci. Technol. A*, 1996, **14**(3), 900–904.
14. Yang, H. M., Luo, J. S. and Lin, W. T., In situ growth of fatigue free $srbi_2ta_2o_9$ films by pulsed laser ablation. *J. Mater. Res.*, 1997, **12**(4), 1145–1151.
15. Desu, S. B., Vijay, D. P., Zhang, X. and He, B. P., Orientation growth of $SrBi_2Ta_2O_9$ ferroelectric thin films. *Appl. Phys. Lett.*, 1996, **69**(12), 1719–1721.
16. Tsai, H. M., Lin, P. and Tseng, T. Y., $Sr_{0.8}Bi_{2.5}Ta_{1.2}Nb_{0.9}O_{9+x}$ ferroelectric thin films prepared by two-target off-axis radio frequency magnetron sputtering. *Appl. Phys. Lett.*, 1998, **72**(14), 1787–1789.
17. Amanuma, K., Hase, T. and Miyasaka, Y., Preparation and ferroelectric properties of $SrBi_2Ta_2O_9$ thin films. *Appl. Phys. Lett.*, 1995, **66**(2), 221–223.
18. Chu Jr., P., Jones, R. E., Zurcher, P., Taylor, D. J., Jiang, B., Gillespie, S. L. and Lii, Y. T., Characteristic of spin-on ferroelectric $SrBi_2Ta_2O_9$ thin film capacitor for FERAM applications. *J. Mater. Res.*, 1996, **11**(5), 1065–1069.
19. Lu, C. H. and Fang, B. K., Secondary phase formation and microstructural development in the interaction between $SrBi_2Ta_2O_9$ films and $Pt/Ti/SiO_2/Si$ substrates. *J. Mater. Res.*, 1997, **12**(8), 2104–2110.
20. Li, T., Zhu, Y., Desu, S. B., Peng, C. H. and Nagata, M., Metal-organic chemical vapor deposition of ferro electric $SrBi_2Ta_2O_9$ thin films. *Appl. Phys. Lett.*, 1996, **68**(5), 616–619.
21. Boyle, T. J., Buchheit, C. D., Rodriguez, M. A., Al-Shareef, H. N., Hernandez, Scott B. A. B. and Ziller, J. W., Formation of SBT: part I, synthesis and characterization of a noval "sol-gel" solution for production of ferroelectric $SrBi_2Ta_2O_9$ thin films. *J. Mater. Res.*, 1996, **11**(9), 2274–2281.
22. Das, R. N., Pathak, A. and Pramanik, P., Low temperature preparation of nanocrystalline lead zirconate titanate and lead lanthanum zirconate titanate powders using triethanolamine. *J. Am. Ceram. Soc.*, 1998, **81**(12), 3357–3360.
23. Roy, J. C., Pati, R. K. and Pramanik, P., Chemical synthesis and cheractarization of nanocrystalline powders of pure zirconia and yttria stabilized zirconia. *J. Eur. Ceram. Soc.*, 2000, **20**, 1289–1295.
24. Wen, W., Yu, Z., Sheng, C., Feng, Y. and Dechang, J., Preparation of strontium bismuth tantalum (SBT) fine powder by sol-gel process using bismuth subnitrate as bismuth source. *Journal of Materials Science & Technology (Shenyang, China)*, 2001, **17**(1), 25–26.
25. Ravichandran, D., Yamakawa, K., Bhalla, A. S. and Roy, R., Alkoxide derived $SrBi_2Ta2O9$ phase pure powder and thin films. *Journal of Sol-Gel Science and Technology*, 1997, **9**(1), 95–101.
26. Lu, C. H. and Saha, S. K., Colloid emulsion of nanosized strontium bismuth tantalate powder. *J. Am. Ceram. Soc.*, 2000, **83**(5), 1320–1322.
27. Nelis, D., Werde, K. V., Mondelaers, D., Vanholand, G., Bael, M. K. V., Mullens, J. and Poucke, L. C. V., Synthesis of $SrBi_2Ta_2O_9$ (SBT) by means of a soluble Ta(V) precursor. *J. Eur. Ceram. Soc.*, 2001, **21**, 2047–2049.
28. Das, R. N. and Pramanik, P., Single step chemical synthesis of lead based relaxor ferroelectric niobate fine powders. *Nano-Structured Materials*, 1999, **11**(3), 325–330.
29. Fairbrother, F., *The Chemistry of Niobium And Tantalum*. Elsevier, London, 1967.
30. tton, F. A. and Willkinson, X., *Inorganic Chemistry*, 5th edition, 1988, Wiley-Interscience.
31. Klug, M. P. and Alexander, L. E., *X-Ray Diffraction Procedure for Polycrystalline and Amorphous Material*. Wiley, New York, 1974.
32. Lu, C. H. and Chen, Y. C., Sintering and decomposition of ferroelectric layered perovskite: strontium bismuth tantalate ceramics. *J. Eur. Ceram. Soc.*, 1999, **19**, 2909–2915.
33. Shimakawa, Y., Kubo, Y., Nakagawa, Y., Goto, S., Kamiyama, T., Asano, H. and Izumi, F., Crystal structure and ferroelectric properties of $ABi_2Ta_2O_9$ (A = Ca, Sr and Ba). *Phys. Rev. B*, 2000, **61**(10), 6559–6564.